

Research Article

Insights into Starch Coated Nanozero Valent Iron-Graphene Composite for Cr(VI) Removal from Aqueous Medium

Prasanna Kumarathilaka,¹ Vimukthi Jayaweera,² Hasintha Wijesekara,¹ I. R. M. Kottegoda,² S. R. D. Rosa,³ and Meththika Vithanage¹

¹Chemical and Environmental Systems Modeling Research Group, National Institute of Fundamental Studies, Kandy, Sri Lanka

²Materials Technology Section, Industrial Technology Institute, Colombo 07, Sri Lanka

³Department of Physics, University of Colombo, Colombo 03, Sri Lanka

Correspondence should be addressed to Meththika Vithanage; meththikavithanage@gmail.com

Received 23 April 2016; Revised 24 August 2016; Accepted 7 September 2016

Academic Editor: Jayavant L. Gunjakar

Copyright © 2016 Prasanna Kumarathilaka et al. This is an open access article distributed under the Creative Commons Attribution License, which permits unrestricted use, distribution, and reproduction in any medium, provided the original work is properly cited.

Embedding nanoparticles into an inert material like graphene is a viable option since hybrid materials are more capable than those based on pure nanoparticulates for the removal of toxic pollutants. This study reports for the first time on Cr(VI) removal capacity of novel starch stabilized nanozero valent iron-graphene composite (NZVI-Gn) under different pHs, contact time, and initial concentrations. Starch coated NZVI-Gn composite was developed through borohydrate reduction method. The structure and surface of the composite were characterized by scanning electron microscopy (SEM), X-ray diffraction spectroscopy (XRD), Fourier transform infrared spectroscopy (FTIR), Brunauer-Emmett-Teller (BET), and point of zero charge (pHpzc). The surface area and pHpzC of NZVI-Gn composite were reported as $525 \text{ m}^2 \text{ g}^{-1}$ and 8.5, respectively. Highest Cr(VI) removal was achieved at pH 3, whereas 67.3% was removed within first few minutes and reached its equilibrium within 20 min obeying pseudo-second-order kinetic model, suggesting chemisorption as the rate limiting process. The partitioning of Cr(VI) at equilibrium is perfectly matched with Langmuir isotherm and maximum adsorption capacity of the NZVI-Gn composite is 143.28 mg g^{-1} . Overall, these findings indicated that NZVI-Gn composite could be utilized as an efficient and magnetically separable adsorbent for removal of Cr(VI).

1. Introduction

Chromium generally exists as the earth's sixth most prominent transition metal [1]. Chromite (FeCr_2O_4), crocoite (PbCrO_4), and chrome ochre (Cr_2O_3) are some of the naturally occurring chromium sources on earth [2]. Both natural and anthropogenic activities may release Cr into surrounding environment. Ultramafic soils such as serpentine may release Cr into water [3, 4]. Many different types of anthropogenic uses such as leather tanning, electroplating, manufacturing of various alloys, mining, cement, metal processing, textile, wood preservation, production of paint pigments, and dye are responsible for releasing Cr into the environment [5, 6].

Chromium contamination in water results from its two stable oxidation forms, Cr(III) and Cr(VI) [7]. In terms of chemical and toxicological characteristics, each form of

Cr has unique properties relative to each other. Cr(III) is less toxic and can form complexes with hydroxides at typical groundwater pH to form Cr(OH)_3 , making it immobile [8]. Cr(III) is one of the essential trace elements in human metabolism and it regulates blood glucose and cholesterol levels [9]. Cr(VI) is highly soluble and extremely mobile in hydrosphere [10]. Human exposure of Cr(VI) at high doses results in liver and kidney damage, diarrhea, nausea, dermatitis, respiratory problems, irritation, and ulceration of the nasal septum [11]. In comparison, Cr(VI) is about 300 times more toxic than Cr(III) and is categorized as carcinogenic and mutagenic [12]. Taking the toxicity into consideration, United States Environmental Protection Agency (USEPA) has established the regulations for discharge of Cr(VI) and total Cr into surface water to be below 0.5 and 2 mg L^{-1} . Further, maximum permissible level of total Cr in drinking water has

been set as $100 \mu\text{g L}^{-1}$ by USEPA [13], whereas World Health Organization (WHO) has set total Cr in drinking water as $50 \mu\text{g L}^{-1}$ [14].

Unlike most of organic pollutants, metal ions including chromium are not easily biodegradable and hence can accumulate throughout the food chain [15]. Many techniques such as chemical precipitation, ultrafiltration, ion exchange, constructed wetlands, adsorption, and reverse osmosis have been developed for removing such metal ions from aqueous medium [16–18]. Mohan et al. [9] have studied the Cr(VI) remediation from water using oak wood and oak bark chars produced from fast pyrolysis. Maximum uptake of 312.52 mg g^{-1} of Cr(VI) by agricultural waste “maize bran” was observed by Hasan et al. [19]. Further, anion exchange resin of DEX-Cr has been successfully used to remove Cr(VI) and maximum removal was achieved at pH of 3 [20].

Recently, iron nanostructures have gained good reputation as highly efficient material for the remediation of various heavy metal ions [21, 22]. Nevertheless, the easy oxidation and rapid agglomeration result in major challenges when using these nanomaterials [23]. To overcome these challenges, embedding nanoparticles into some inert material like graphene is a viable option [24, 25]. The term “graphene” is defined as a single carbon layer of the graphite structure [26]. Owing to unique and extraordinary properties such as a large dimension in XY plane, large specific area, and high degree of sp^2 -bonded carbon region, graphene is able to retain and well disperse the nanoparticles [27]. Additionally, superior conductivity of graphene provides more efficient electron transfer between nanoparticles and targeted pollutant [26]. In this sense, graphene-based nanomaterials have become the focus of many researches [28, 29].

Several studies have been conducted for graphene nanoparticle composites for environmental remediation. A study by Wang et al. [30] revealed that nanoscale zero valent iron reduced graphite oxide composite successfully and removed As(III) and As(V) from the aqueous solution with a capacity of 35.83 and 29.04 mg g^{-1} , respectively. Recently, NZVI-Gn composite was found to be well adsorbing Co(II) with a capacity of 131.58 mg g^{-1} [31]. Amongst the studies, one study reports that the NZVI-Gn composite removes Pb(II) ions with adsorption capacity of 181.04 mg g^{-1} ; however, the authors have used non-stabilized NZVI to form the graphene composite [24]. Such NZVI can quickly be oxidized due to its strong oxidizing ability and no coating is present to prevent it. Hence, it is better to use a coated NZVI so that it may not oxidize fast and that will lead to a higher reaction capacity [22]. Stabilizing agents such as starch would act as a strong foundation for preventing oxidation probability of NZVI. Therefore, making a composite by using starch stabilized NZVI could be a viable option in terms of stability compared to the nonstabilized materials under environmental conditions. There is little available information on Cr(VI) removal by stabilized NZVI-Gn composite. However, a study by Jabeen et al. [23] reveled that NZVI-Gn composite, in which NZVI was not coated by a stabilizing material, successfully removed Cr(VI) from aqueous medium with adsorption capacity of 162.59 mg g^{-1} . Take into account, in this work,

that stabilized NZVI-Gn composite was produced to examine the ability to remove Cr(VI) from aqueous solution. For that, graphite oxide was firstly prepared via chemically oxidized method and then NZVI-Gn composite, of which NZVI was coated by starch, was developed through NaBH_4 reduction method. The composite was characterized by SEM, XRD, FTIR, BET, and pHpzc. After that, the ability of NZVI-Gn composite for Cr(VI) removal from aqueous medium was examined under different pH values, contact time, and initial Cr(VI) concentrations.

2. Materials and Methods

2.1. Preparation of Graphene Oxide (GO). The vain graphite powder from Kahatagaha ore in Sri Lanka (99.9% purity, $\leq 38 \mu\text{m}$) was oxidized using the concentrated acid mixture of H_2SO_4 and 40% H_3PO_4 (9:1 volume ratio). After that, 3 g graphite flakes and 18 g of KMnO_4 were gradually added to the mixture [32]. The reaction mixture was then heated at 50°C with continuous agitation overnight. After cooling, 500 g of ice and 5 mL of 30% H_2O_2 were added and the mixture was centrifuged. The suspended solid material was then washed in succession two times by water, 30% HCl, ethanol, and ether. After washing, suspension was vacuum dried overnight at 60°C to obtain the solid graphite oxide.

2.2. Synthesis of the NZVI-Gn. NZVI-Gn was synthesized according to the method described by Wijesekara et al. [22] with some modifications. 100 mL of 0.5 M sodium borohydride solution (made from NaBH_4) was added dropwise into a flask containing 100 mL of 0.14 M ferrous sulfate solution (made from $\text{FeSO}_4 \cdot 7\text{H}_2\text{O}$) to reduce Fe(II). Synthesis was done under continuous stirring in inert environment. Borohydride addition was completed in $\sim 2\text{ h}$ to control particle size. In addition, 50 mg of graphite oxide and 5% (w/w) starch were added to the ferrous sulfate solution. An additional 10 mL sodium borohydride was added and the mixture was stirred under a nitrogen gas flow to avoid dissolving oxygen for 15 min to complete the reaction. The precipitated NZVI-Gn slurries were transferred to the centrifuged tubes and sealed them with parafilm immediately inside the chamber. Then, the NZVI-Gn particles were separated by centrifugation at 2500 rpm for 10 min and washed by resuspending the material in absolute ethanol. This procedure was repeated three times. After the final centrifugation, composites were dried in a freeze dryer for approximately 45 min, and prepared composites were stored below 4°C . Figure 1 illustrates the way in which NZVI-Gn composite was produced. Further, it is observed that synthesized NZVI-Gn composite was magnetically separable (Figures 2(a) and 2(b)).

2.3. Characterization. The morphologies of developed NZVI-Gn composite were characterized by SEM (FEI Quanta 200 environmental scanning electron microscope) and scanning electron microscopy combined with electron dispersive spectroscopy (SEM-EDX) analyzed elemental mapping of the NZVI-Gn composite. XRD patterns were obtained using a Regaku Ultima VI X-ray diffractometer using $\text{Cu } K_\alpha$ ($\lambda = 1542 \text{ \AA}$) radiation. FTIR spectra were

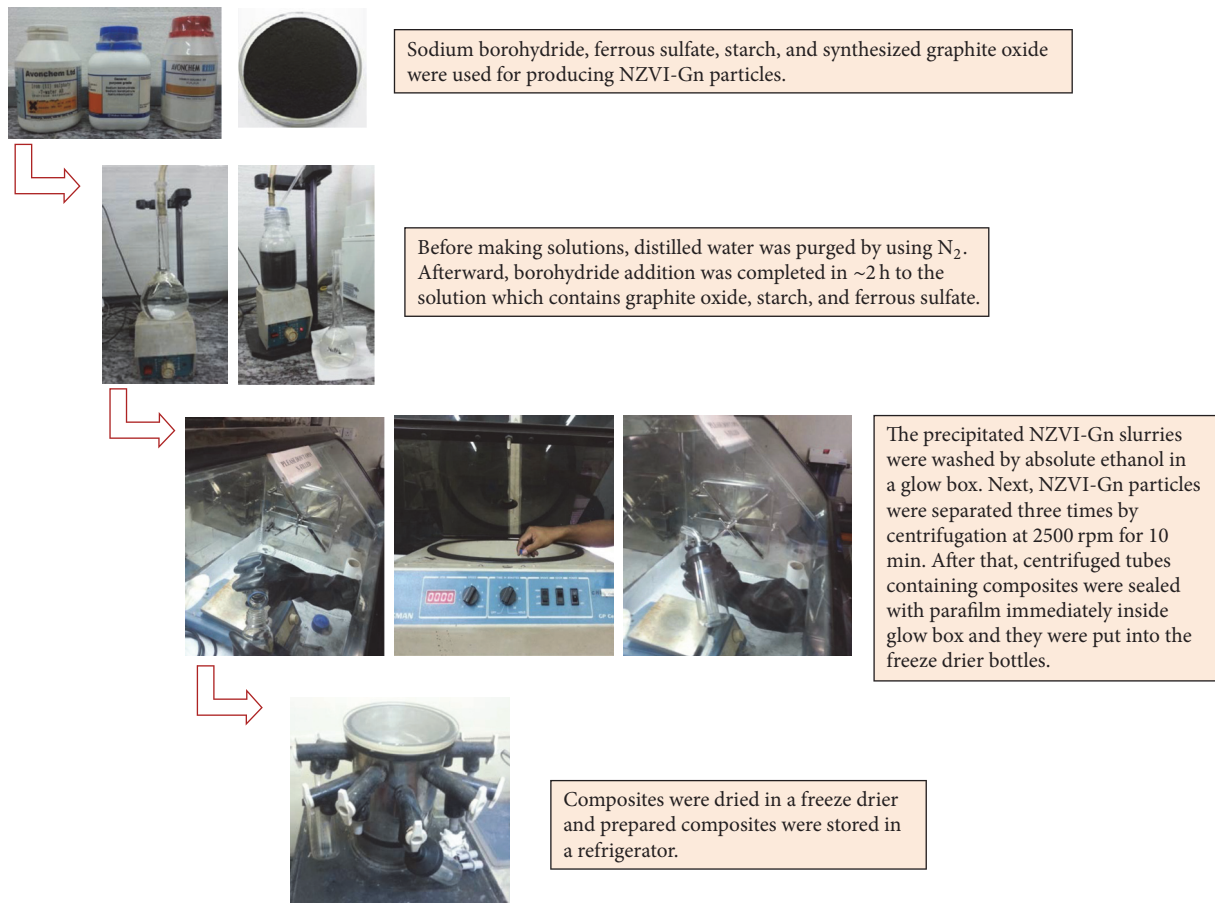


FIGURE 1: Schematic representation of synthesis of NZVI-Gn composite.

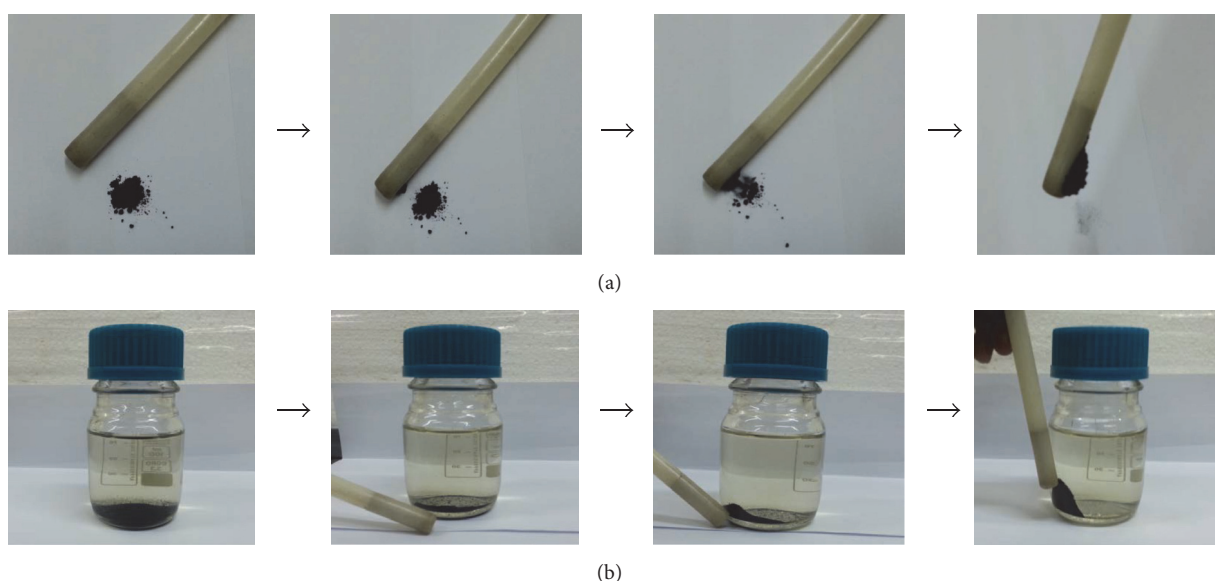


FIGURE 2: (a) and (b) Stepwise process indicates how synthesized NZVI-Gn composite interacts towards the magnet pole.

obtained using a FTIR spectrometer (BRUKER Tenor 27 FTIR-ATR). BET was studied to measure the specific surface area of the NZVI-Gn composite and measurements were obtained using a surface area analyzer. Surface titration was carried out to determine pH_{pzc} of the NZVI-Gn composite.

2.4. Chromium (VI) Removal by the Composite. Potassium dichromate ($K_2Cr_2O_7$) was purchased from Vickers Laboratories, UK. All experiments were performed in duplicate and under nitrogen atmosphere. The preliminary experiments were conducted for the pH range of 3 to 9 and desired pH value was adjusted by adding nitric acid or sodium hydroxide solutions. For the kinetic study, the concentrations of the NZVI-Gn were maintained at 0.25 g L^{-1} and initial Cr(VI) solution concentration was kept in 50 mg L^{-1} with initial pH value of 3. The mixed solutions were stirred on a mechanical shaker (EYELA B603 shaker) with a shaking speed of 100 rpm at room temperature ($\sim 25^\circ\text{C}$). Aliquots of samples were taken at certain time intervals, 2, 5, 10, 15, 20, 30, 45, and 60 min, and analyzed immediately after being filtered through a $0.45\text{ }\mu\text{m}$ filter membrane. The concentration Cr(VI) was determined by following 1,5-diphenylcarbazide method and absorbance was recorded in UV-Visible Recording Spectrophotometer (UV-160A) at $\lambda = 540\text{ nm}$. The adsorption isotherms were investigated by different models with Cr(VI) concentration ranging from 10 to 60 mg L^{-1} under initial pH value of 3 for 1 h.

3. Results and Discussion

3.1. Characterization of NZVI-Gn Composite. SEM was used to study the morphology of developed NZVI-Gn composite (Figure 3(a)). These images show that the sheet like structure of graphene has been perfectly developed. Apparently, aggregates of zero valent iron nanoparticles are uniformly distributed throughout the smooth graphene surface.

Figure 3(b) reveals the changes in XRD patterns during the development of NZVI-Gn composite. The peak which appeared at 9.65° (001) indicates the successful development of graphene oxide [33]. The peak at $2\theta = 44.71^\circ$ (001) exhibits the formation of the final product, NZVI-Gn composite. Furthermore, the average particle size of the NZVI-Gn composite was found to be 24.17 nm based on Scherrer's equation at the peak at $2\theta = 44.71^\circ$. Figure 4(a) depicts the FTIR spectra of NZVI-Gn composite and GO. The FTIR spectra showed that some peaks were shifted or disappeared and new peaks were also detected. In GO spectrum, absorption peaks at 868, 1037, and 1223 cm^{-1} corresponded to the asymmetric stretching modes of C=C bonds, alkoxy C-O, and epoxy C-O stretches, respectively [23, 34]. The peak at 1407 cm^{-1} can be assigned to COO-symmetric vibration [35], whereas peaks at 1624 and 1731 cm^{-1} correspond to skeletal vibrations of unoxidized graphitic domains (C=C) and C=O stretch in carboxylic acid or carbonyl moieties [36]. The broad absorption peaks at $3000\text{--}3500\text{ cm}^{-1}$ can be attributed to the stretching of O-H. Comparing the spectra before and after oxidation into the NZVI-Gn composite, most of the oxygen containing functional groups disappeared. The absorption peak at 1407 cm^{-1} vanished and absorption intensity around 1630 and 1740 cm^{-1}

decreased, exhibiting the reduction of GO [35]. The new peaks around $2680\text{--}2900\text{ cm}^{-1}$ are corresponding to the stretching vibrations of C-H [34], whereas the peaks at 1131 and 1266 cm^{-1} may be due to the C-O stretch by nonoxidized residual surface oxygen species. The bands which appeared at 678 and 610 cm^{-1} can be attributed to the stretching vibration modes of Fe-O due to surface oxidation of zero valent iron nanoparticles [33].

The BET method indicates that the surface area of NZVI-Gn composite is $525\text{ m}^2\text{ g}^{-1}$. Surface area of the NZVI has been studied by Wijesekara et al. [22] and is reported as $136\text{ m}^2\text{ g}^{-1}$. Hence, it is obvious that zero valent iron decorated graphene sheets increased surface area approximately 4 times greater than NZVI. This enhancement in surface area for NZVI-Gn composite leads to increment of adsorption sites for Cr(VI) removal, as compared with NZVI.

The point of zero charge (pH_{pzc}) is the pH at which the net charge on the surface is zero. This was found to be 8.5 for NZVI-Gn composite tested in this study (Figure 4(b)). When pH_{pzc} < pH of the solution, the NZVI-Gn composite surface will be negatively charged, whereas when the pH_{pzc} > pH of the solution, the surface of the NZVI-Gn tends to be positively charged [37]. To the best of our knowledge, pH_{pzc} of the NZVI-Gn composite was not reported in literature. However, a study by Sun et al. [38] assessed the pH_{pzc} of the NZVI as 8.3.

3.2. Effect of Initial pH. The initial pH of the solution is one of the key indices which determines the existing form of species and sorption behavior of adsorbent [19]. Figure 5(a) shows the variation in the removal efficiency of Cr(VI) by the NZVI-Gn composite as solution pH changed from 3 to 9. Apparently, it is noted that high efficiency of Cr(VI) removal, almost 100%, is achieved in acidic environment. Nevertheless, in alkaline environments, conspicuous decrease of Cr(VI) removal efficiency appeared and eventually fell to 80.84% at initial pH 9. Overall, it is obvious that NZVI-Gn composite is able to remove Cr(VI) in wide pH range to a great extent.

Generally, $HCrO_4^-$ is the most abundant species of Cr(VI) at pH less than 6, whereas $Cr_2O_7^{2-}$ is highly available in concentrated Cr(VI) solutions at highly acidic pH. As pH increases above 6, CrO_4^{2-} and $Cr_2O_7^{2-}$ become the predominant form of Cr(VI). If solution pH rises above 7.5, CrO_4^{2-} is the stable form of Cr(VI) [36]. Hence, influence of solution pH on Cr(VI) removal can be described from the surface chemistry at the interface. Regardless of the prominent forms of Cr(VI), they all are negatively charged in the normal pH range.

More precisely, the pH_{pzc} can be used to explain the effect of pH on the adsorption process. In general, when the pH of solution is below the pH_{pzc}, the surface of the adsorbent is positively charged and it becomes negative if the pH is above the pH_{pzc}. Thereby, it can be suggested that positive surface of NZVI-Gn composite under acidic medium is more attractive for Cr(VI). In other words, when the pH of solution is decreased, the density of the positive charged sites increases possibly due to the electrostatic forces between NZVI-Gn composite and negatively charged Cr(VI) species. Conversely,

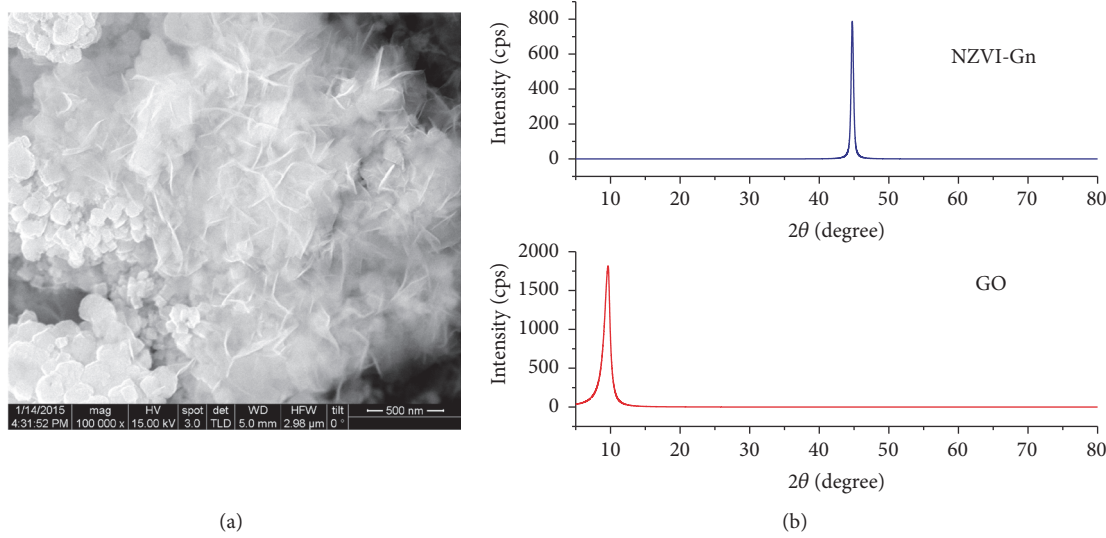


FIGURE 3: (a) SEM image of NZVI-Gn composite. (b) XRD patterns of NZVI-Gn composite and GO which is used to synthesize the composite.

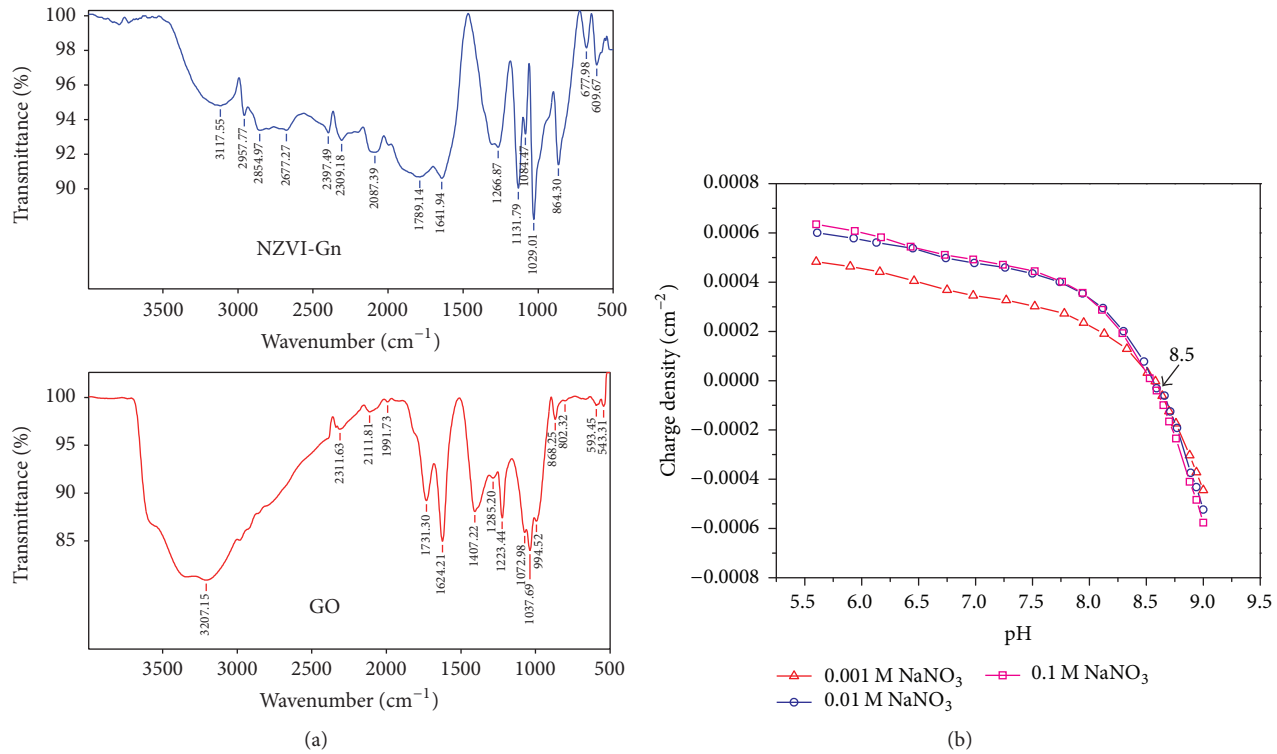


FIGURE 4: (a) FTIR spectra for NZVI-Gn composite and GO. (b) Proton titration curves of NZVI-Gn composite as a function of ionic strength.

at higher pH of solution, density of positive charge sites of NZVI-Gn composite surface decreases and results in slightly low adsorption due to repulsive force between adsorbent and negatively charged adsorbate.

3.3. Sorption Kinetics. It is important to investigate the effect of adsorption kinetics to understand and predict the influence of reaction time on mobility and the retention of

Cr(VI). Figure 5(b) depicts the effects of reaction time on the sorption of Cr(VI) onto NZVI-Gn composite. A rapid sorption of Cr(VI) was observed within first few minutes of contact time, resulting in an adsorption of 123.77 mg g^{-1} (67.3%), and it then reached its equilibrium value within about 20 min. The rapid adsorption at the initial contact time was probably due to the availability of the positively charged surface sites of NZVI-Gn composite for Cr(VI) interaction. In

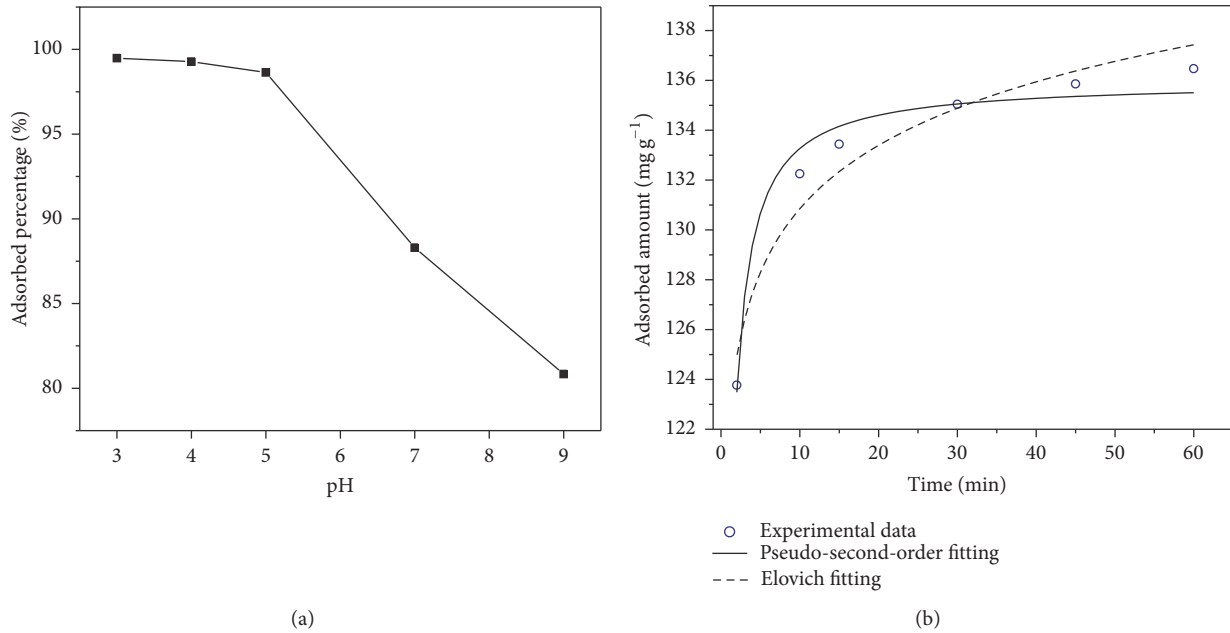


FIGURE 5: (a) Effect of solution pH on Cr(VI) adsorption efficiency. (b) Pseudo-second-order and Elovich kinetic models for Cr(VI) on NZVI-Gn composite at pH 3.

TABLE 1: Comparison of different kinetic models and correlation coefficients (r^2) for Cr(VI) adsorption at pH 3.

Nonlinear model	Equation	Parameter	Value	r^2
Pseudo first order	$q_t = q_e (1 - e^{-k_1 t})$	k_1	1.259	0.889
		q_e	134.61	
Pseudo second order	$q_t = \frac{q_e^2 k_2 t}{1 + k_2 t q_e}$	k_2	0.036	0.974
		q_e	135.96	
Elovich	$q_t = \frac{1}{b} \ln(ab) + \frac{1}{b} \ln(t)$	a	1.095	0.947
		b	0.272	
Parabolic	$q_t = a + k_p \sqrt{t}$	a	124.445	0.787
		k_p	1.767	
Power function	$q_t = b(t^{k_f})$	b	122.683	0.941
		k_f	0.027	

addition, decrease in sorption with time could be attributed to the electrostatic hindrance within the adsorbed negatively charged Cr(VI) onto the surface of NZVI-Gn composite.

Experimental kinetic data were fitted to pseudo-first-order, pseudo-second-order, Elovich, parabolic diffusion, and power function models in order to understand the rate limiting factor. Table 1 summarizes the fitting results obtained from various nonlinear models. It can be noted that kinetics of Cr(VI) adsorption process are described well by the pseudo-second-order nonlinear model compared to other kinetic models applied in this study (Figure 5(b)). The predicted adsorption capacity (q_e) determined by the pseudo-second-order model is 135.96 mg g^{-1} . The pseudo-second-order model is based on the assumption of chemical sorption involving valence forces through sharing or exchange of electrons between the adsorbent and the adsorbate

[9]. The adsorption kinetics best fitted the pseudo-second-order model, suggesting that the adsorption occurs via a chemisorption interaction postulated between Cr(VI) and NZVI-Gn composite. Overall, the correlation coefficient (r^2) values indicated that the best fitting order of kinetic models is determined to be pseudo-second-order > Elovich > power function > pseudo-first-order > parabolic diffusion. The experimental data secondly fitted well to the Elovich model, further confirming that Cr(VI) adsorption onto NZVI-Gn composite could be more inclined towards chemisorption mechanism.

3.4. Adsorption Isotherm and Distribution Coefficient. The adsorption equilibrium data were correlated with different types of adsorption isotherm models. Table 2 summarizes the

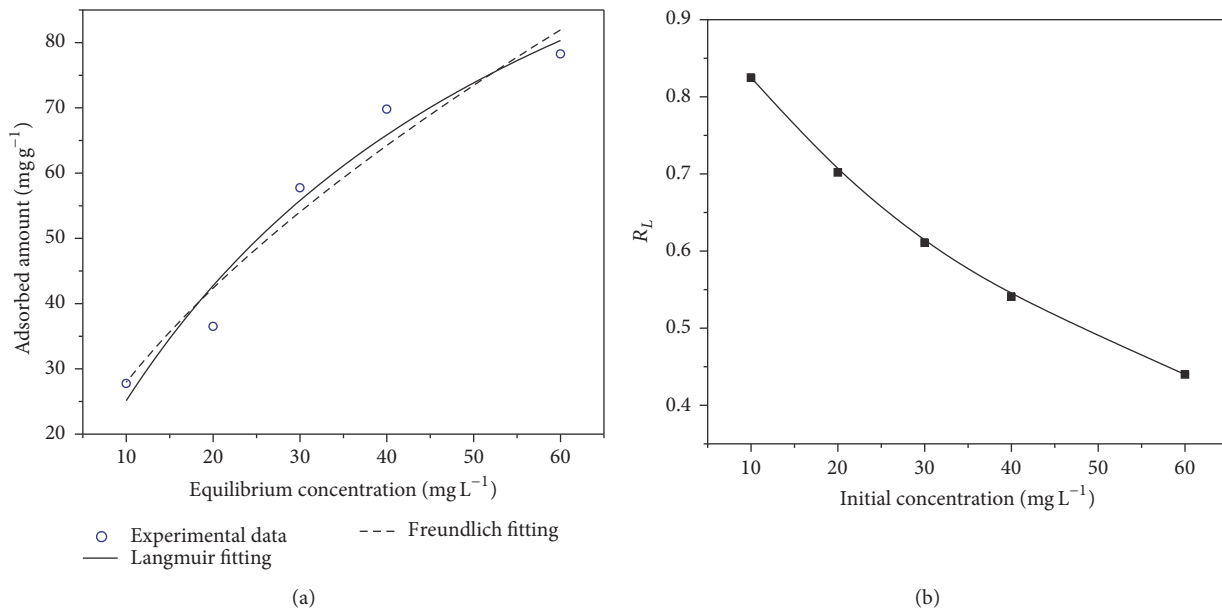


FIGURE 6: (a) Cr(VI) sorption isotherms for NZVI-Gn composite at pH 3. (b) Values of the Langmuir separation factor, R_L , for NZVI-Gn composite at pH 3.

TABLE 2: Saturation capacities, Langmuir, Freundlich, Temkin and Dubinin–Radushkevish isotherm parameters and correlation coefficients (r^2) for Cr(VI) adsorption onto NZVI-Gn composite at pH 3.

Model	Nonlinear equation	Description	Isotherm parameters	Value	r^2
Langmuir	$q_{\text{ads}} = \frac{q_{\max} K_L C_e}{1 + K_L C_e}$	q_{ads} (mg g ⁻¹): amount of adsorbate adsorbed per unit weight of adsorbent q_{\max} (mg g ⁻¹): maximum adsorption capacity K_L (L mg ⁻¹): Langmuir affinity parameter C_e (mg L ⁻¹): equilibrium adsorbate aqueous phase concentration	q_{\max} (mg g ⁻¹) K_L (L g ⁻¹)	143.28 0.021	0.962
Freundlich	$q_{\text{ads}} = K_F C_e^n$	K_F ((mg g ⁻¹)/(mg L ⁻¹) ⁿ): Freundlich affinity-capacity parameter n : Freundlich exponent	K_F ((mg g ⁻¹)/(mg L ⁻¹) ⁿ) n	7.01 1.66	0.949
Temkin	$q_{\text{ads}} = \frac{RT}{b} \ln(AC_e)$	R : universal gas constant (8.314 J K ⁻¹ mol ⁻¹) T : absolute temperature (K) b : heat of adsorption (J) A : binding constant (L mg ⁻¹)	A (L mg ⁻¹) b	0.21 81.29	0.948
Dubinin- Radushkevish	$q_{\text{ads}} = q_D \exp\left(-B_D \left[RT \ln\left(1 + \frac{1}{C_e}\right)\right]^2\right)$	q_D : monolayer adsorption capacity (mg g ⁻¹) B_D : mean free energy of sorption (mol ² K ⁻¹)	q_D (mg g ⁻¹) B_D (mol ² K ⁻¹)	73.46 0.00	0.789

details of nonlinear isotherm models and the related parameters. r^2 for Langmuir, Freundlich, Temkin, and Dubinin–Radushkevich models are of 0.962, 0.949, 0.948, and 0.789, respectively. In fact, the higher r^2 value indicates a best applicable model to isotherm of Cr(VI) adsorption; Langmuir isotherm model can be considered as the perfectly matched model to describe the sorption of Cr(VI) on NZVI-Gn composite (Figure 6(a)). Langmuir model suggested that the adsorption of Cr(VI) occurs on a homogeneous surface by

monolayer adsorption, and no interaction happens between adsorbed species [39]. Maximum adsorption capacity (q_{\max}) determined by Langmuir model was 143.28 mg g⁻¹.

The essential characteristics of Langmuir isotherm can be defined in terms of dimensionless constant separation factor, R_L , as in the following equation:

$$R_L = \frac{1}{(1 + bC_o)}, \quad (1)$$

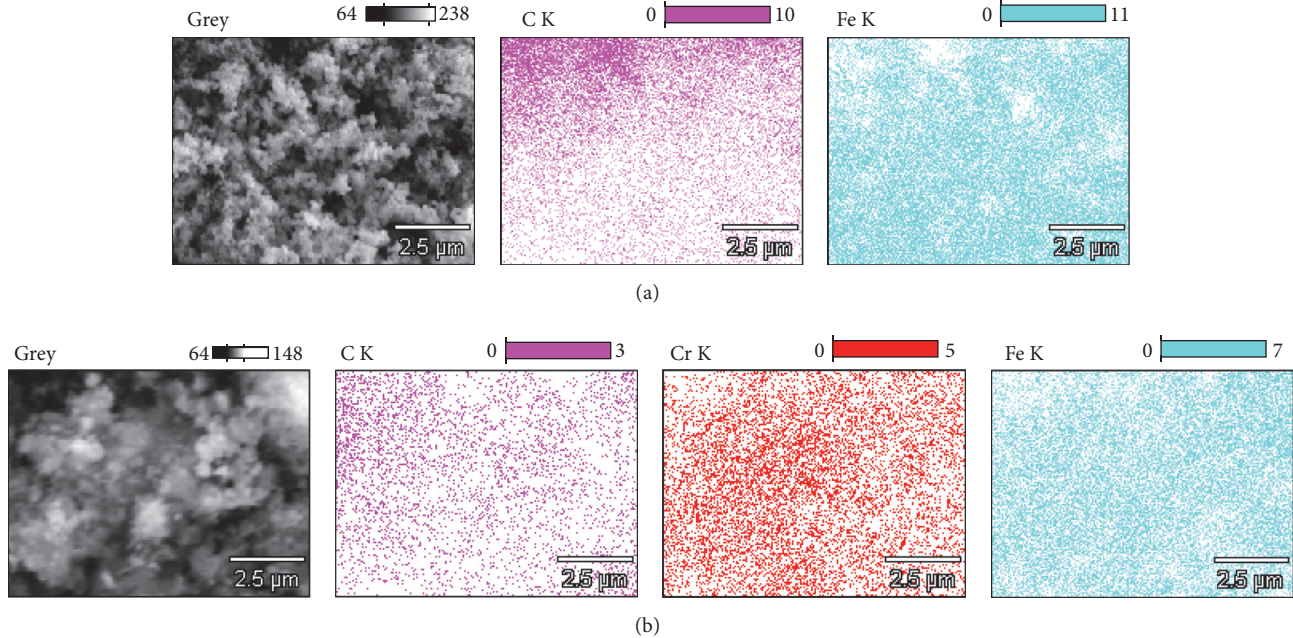


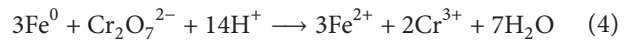
FIGURE 7: SEM-EDX mapping for the NZVI-Gn composite (a) before the Cr(VI) removal and (b) after the Cr(VI) adsorption.

where b is the Langmuir constant and C_o is the initial Cr(VI) concentration in mg L^{-1} . Commonly, the value of $R_L > 1$ adsorption is unfavorable, $R_L = 1$ adsorption is linear, $0 < R_L < 1$ adsorption is favorable, and $R_L = 0$ adsorption is irreversible [40]. Figure 6(b) illustrates the variation in R_L values for the adsorption of Cr(VI) by NZVI-Gn composite. The reported R_L values in this study were <1 , confirming the favorable sorption in agreement with Langmuir model assumptions.

3.5. Possible Mechanisms for Cr(VI) Removal. Figures 7(a) and 7(b) show SEM-EDX elemental mapping of NZVI-Gn composites before and after Cr(VI) adsorption and they clearly indicate the Cr(VI) adsorption onto the composite surface. Before the Cr(VI) adsorption, atomic percentages for carbon and iron in NZVI-Gn composite were 69.26 and 30.74%, respectively. However, after the Cr(VI) treatment, the percentage of carbon and iron in NZVI-Gn composite declined to 50.91 and 40.78, respectively, and it is followed by chromium with 8.31%, indicating successful adsorption of Cr(VI).

The possible mechanism of Cr(VI) removal is schematically described in Figure 8. At the beginning, $\text{Fe}(0)$ may be oxidized to $\text{Fe}(\text{II})$ while reducing $\text{Cr}_2\text{O}_7^{2-}$ into $\text{Cr}(\text{III})$ (see (2), (3), and (4)). This redox reaction is highly favorable at highly acidic pHs, since $\text{Fe}(\text{II})$ state becomes dominated at low pHs. Further, the extraordinary electrical conductivity of graphene sheets enhances quick and continuous electron transfer [33] and, subsequently, high BET surface area of NZVI-Gn composite facilitates abundant sites for Cr(VI) to capture electrons [26]. Consequently, free Cr(VI) and Cr(III) forms could be immobilized on the graphene sheets through

π electron and cation interactions. Taking the above into consideration, it can be suggested that adsorption and reduction of free Cr(VI) ions by NZVI followed by immobilization on the graphene sheets may enhance the removal of Cr(VI) from aqueous medium.



4. Conclusions

In summary, the ability of Cr(VI) reduction and removal using novel NZVI-Gn composites were studied. The composite was characterized by SEM, XRD, FTIR, BET, and pHPzc and the NZVI was found to be homogeneously impregnated onto graphene sheets with high surface area. The results revealed that NZVI-Gn composite achieved excellent removal efficiency under acidic environment. Kinetic study suggested that pseudo-second-order adsorption model is suitable to explain the adsorption behavior of NZVI-Gn composite so that the rate limiting factor could be a chemisorption process. Langmuir isotherm model provided a better correlation of the experimental equilibrium data, suggesting that the adsorption of Cr(VI) onto NZVI-Gn composite may involve a mono-layer process. More precisely, dual sorption and reduction followed by immobilization process may enhance Cr(VI) removal to a great extent. Thereby, the prepared NZVI-Gn composites provide an admirable alternative as an efficient and magnetically separable adsorbent for Cr(VI) removal from the environment.

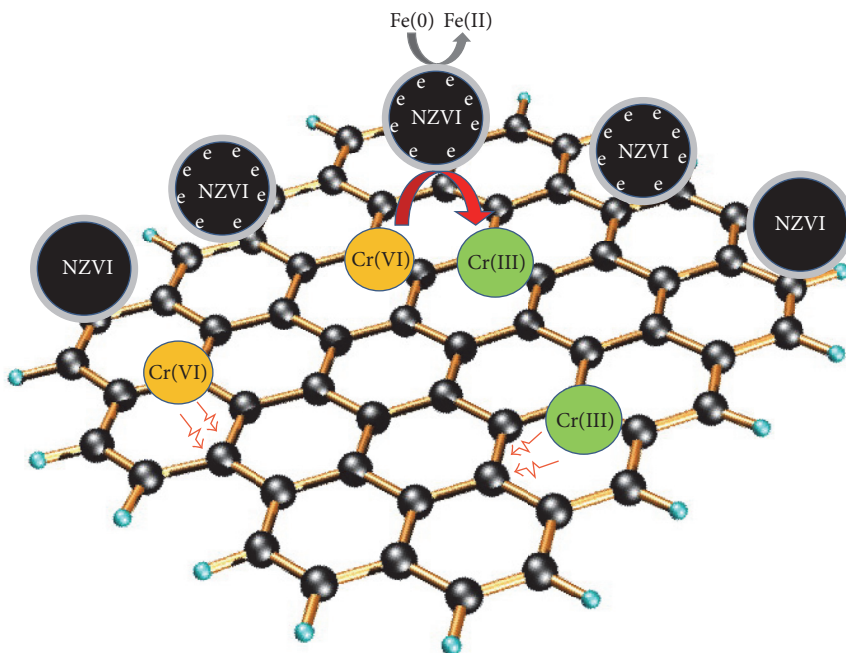


FIGURE 8: Graphical representation of possible mechanisms for monolayer Cr(VI) adsorption onto NZVI-Gn composite.

Competing Interests

The authors declare that they have no competing interests.

References

- [1] D. Mohan and C. U. Pittman Jr., "Activated carbons and low cost adsorbents for remediation of tri- and hexavalent chromium from water," *Journal of Hazardous Materials*, vol. 137, no. 2, pp. 762–811, 2006.
- [2] D. Mohan, K. P. Singh, and V. K. Singh, "Removal of hexavalent chromium from aqueous solution using low-cost activated carbons derived from agricultural waste materials and activated carbon fabric cloth," *Industrial & Engineering Chemistry Research*, vol. 44, no. 4, pp. 1027–1042, 2005.
- [3] A. U. Rajapaksha, M. Vithanage, C. Oze, W. M. A. T. Bandara, and R. Weerasooriya, "Nickel and manganese release in serpentine soil from the Ussangoda ultramafic complex, Sri Lanka," *Geoderma*, vol. 189–190, pp. 1–9, 2012.
- [4] M. Vithanage, A. U. Rajapaksha, C. Oze, N. Rajakaruna, and C. B. Dissanayake, "Metal release from serpentine soils in Sri Lanka," *Environmental Monitoring and Assessment*, vol. 186, no. 6, pp. 3415–3429, 2014.
- [5] A. Zhitkovich, "Chromium in drinking water: sources, metabolism, and cancer risks," *Chemical Research in Toxicology*, vol. 24, no. 10, pp. 1617–1629, 2011.
- [6] B. Dhal, H. N. Thatoi, N. N. Das, and B. D. Pandey, "Chemical and microbial remediation of hexavalent chromium from contaminated soil and mining/metallurgical solid waste: a review," *Journal of Hazardous Materials*, vol. 250–251, pp. 272–291, 2013.
- [7] E. Kaprara, N. Kazakis, K. Simeonidis et al., "Occurrence of Cr(VI) in drinking water of Greece and relation to the geological background," *Journal of Hazardous Materials*, vol. 281, pp. 2–11, 2015.
- [8] V. Lugo-Lugo, L. A. Bernal-Martínez, F. Ureña-Núñez, I. Linares-Hernández, P. T. Almazán-Sánchez, and P. J. B. De Vázquez-Santillán, "Treatment of Cr(VI) present in plating wastewater using a Cu/Fe galvanic reactor," *Fuel*, vol. 138, pp. 203–214, 2014.
- [9] D. Mohan, S. Rajput, V. K. Singh, P. H. Steele, and C. U. Pittman Jr., "Modeling and evaluation of chromium remediation from water using low cost bio-char, a green adsorbent," *Journal of Hazardous Materials*, vol. 188, no. 1–3, pp. 319–333, 2011.
- [10] L. A. Hellerich and N. P. Nikolaidis, "Studies of hexavalent chromium attenuation in redox variable soils obtained from a sandy to sub-wetland groundwater environment," *Water Research*, vol. 39, no. 13, pp. 2851–2868, 2005.
- [11] M. Cieślak-Golonka, "Toxic and mutagenic effects of chromium(VI). A review," *Polyhedron*, vol. 15, no. 21, pp. 3667–3689, 1996.
- [12] B. R. Araújo, J. O. M. Reis, E. I. P. Rezende et al., "Application of termite nest for adsorption of Cr(VI)," *Journal of Environmental Management*, vol. 129, pp. 216–223, 2013.
- [13] A. Baral and R. D. Engelen, "Chromium-based regulations and greening in metal finishing industries in the USA," *Environmental Science and Policy*, vol. 5, no. 2, pp. 121–133, 2002.
- [14] WHO, *Chromium in Drinking-Water*, World Health Organization, Geneva, Switzerland, 1996.
- [15] C. E. Barrera-Díaz, V. Lugo-Lugo, and B. Bilyeu, "A review of chemical, electrochemical and biological methods for aqueous Cr(VI) reduction," *Journal of Hazardous Materials*, vol. 223–224, pp. 1–12, 2012.
- [16] H. Demiral, I. Demiral, F. Tümsek, and B. Karabacakoglu, "Adsorption of chromium(VI) from aqueous solution by activated carbon derived from olive bagasse and applicability of different adsorption models," *Chemical Engineering Journal*, vol. 144, no. 2, pp. 188–196, 2008.

- [17] S. Edebali and E. Pehlivan, "Evaluation of Amberlite IRA96 and Dowex 1×8 ion-exchange resins for the removal of Cr(VI) from aqueous solution," *Chemical Engineering Journal*, vol. 161, no. 1-2, pp. 161–166, 2010.
- [18] G. Ghosh and P. K. Bhattacharya, "Hexavalent chromium ion removal through micellar enhanced ultrafiltration," *Chemical Engineering Journal*, vol. 119, no. 1, pp. 45–53, 2006.
- [19] S. H. Hasan, K. K. Singh, O. Prakash, M. Talat, and Y. S. Ho, "Removal of Cr(VI) from aqueous solutions using agricultural waste 'maize bran,'" *Journal of Hazardous Materials*, vol. 152, no. 1, pp. 356–365, 2008.
- [20] X. Liu, Y. Li, C. Wang, and M. Ji, "Cr (VI) removal by a new type of anion exchange resin DEX-Cr: adsorption affecting factors, isotherms, kinetics, and desorption regeneration," *Environmental Progress and Sustainable Energy*, vol. 34, no. 2, pp. 387–393, 2015.
- [21] X.-Q. Li, D. W. Elliott, and W.-X. Zhang, "Zero-valent iron nanoparticles for abatement of environmental pollutants: materials and engineering aspects," *Critical Reviews in Solid State and Materials Sciences*, vol. 31, no. 4, pp. 111–122, 2006.
- [22] S. S. R. M. D. H. R. Wijesekara, B. F. A. Basnayake, and M. Vithanage, "Organic-coated nanoparticulate zero valent iron for remediation of chemical oxygen demand (COD) and dissolved metals from tropical landfill leachate," *Environmental Science and Pollution Research*, vol. 21, no. 11, pp. 7075–7087, 2014.
- [23] H. Jabeen, V. Chandra, S. Jung, J. W. Lee, K. S. Kim, and S. B. Kim, "Enhanced Cr(VI) removal using iron nanoparticle decorated graphene," *Nanoscale*, vol. 3, no. 9, pp. 3583–3585, 2011.
- [24] H. Jabeen, K. C. Kemp, and V. Chandra, "Synthesis of nano zerovalent iron nanoparticles—graphene composite for the treatment of lead contaminated water," *Journal of Environmental Management*, vol. 130, pp. 429–435, 2013.
- [25] J. Guo, R. Wang, W. W. Tjiu, J. Pan, and T. Liu, "Synthesis of Fe nanoparticles@graphene composites for environmental applications," *Journal of Hazardous Materials*, vol. 225–226, pp. 63–73, 2012.
- [26] S. Chowdhury and R. Balasubramanian, "Recent advances in the use of graphene-family nanoadsorbents for removal of toxic pollutants from wastewater," *Advances in Colloid and Interface Science*, vol. 204, pp. 35–56, 2014.
- [27] J. Zhu, S. Wei, H. Gu et al., "One-pot synthesis of magnetic graphene nanocomposites decorated with core@double-shell nanoparticles for fast chromium removal," *Environmental Science and Technology*, vol. 46, no. 2, pp. 977–985, 2012.
- [28] S. Wang, H. Sun, H. M. Ang, and M. O. Tadé, "Adsorptive remediation of environmental pollutants using novel graphene-based nanomaterials," *Chemical Engineering Journal*, vol. 226, pp. 336–347, 2013.
- [29] R. Alam, I. V. Lightcap, C. J. Karwacki, and P. V. Kamat, "Sense and shoot: simultaneous detection and degradation of low-level contaminants using graphene-based smart material assembly," *ACS Nano*, vol. 8, no. 7, pp. 7272–7278, 2014.
- [30] C. Wang, H. Luo, Z. Zhang, Y. Wu, J. Zhang, and S. Chen, "Removal of As(III) and As(V) from aqueous solutions using nanoscale zero valent iron-reduced graphite oxide modified composites," *Journal of Hazardous Materials*, vol. 268, pp. 124–131, 2014.
- [31] M. Xing, L. Xu, and J. Wang, "Mechanism of Co(II) adsorption by zero valent iron/graphene nanocomposite," *Journal of Hazardous Materials*, vol. 301, pp. 286–296, 2016.
- [32] D. C. Marcano, D. V. Kosynkin, J. M. Berlin et al., "Improved synthesis of graphene oxide," *ACS Nano*, vol. 4, no. 8, pp. 4806–4814, 2010.
- [33] X. Lv, X. Xue, G. Jiang et al., "Nanoscale Zero-Valent Iron (nZVI) assembled on magnetic Fe_3O_4 /graphene for Chromium (VI) removal from aqueous solution," *Journal of Colloid and Interface Science*, vol. 417, pp. 51–59, 2014.
- [34] C. Li, Y. Dong, J. Yang, Y. Li, and C. Huang, "Modified nano-graphite/ Fe_3O_4 composite as efficient adsorbent for the removal of methyl violet from aqueous solution," *Journal of Molecular Liquids*, vol. 196, pp. 348–356, 2014.
- [35] T. Qi, C. Huang, S. Yan, X.-J. Li, and S.-Y. Pan, "Synthesis, characterization and adsorption properties of magnetite/reduced graphene oxide nanocomposites," *Talanta*, vol. 144, pp. 1116–1124, 2015.
- [36] L. Zhou, H. Deng, J. Wan, J. Shi, and T. Su, "A solvothermal method to produce RGO- Fe_3O_4 hybrid composite for fast chromium removal from aqueous solution," *Applied Surface Science*, vol. 283, pp. 1024–1031, 2013.
- [37] M. Essandoh, B. Kunwar, C. U. Pittman Jr., D. Mohan, and T. Mlsna, "Sorptive removal of salicylic acid and ibuprofen from aqueous solutions using pine wood fast pyrolysis biochar," *Chemical Engineering Journal*, vol. 265, pp. 219–227, 2015.
- [38] Y.-P. Sun, X.-Q. Li, J. Cao, W.-X. Zhang, and H. P. Wang, "Characterization of zero-valent iron nanoparticles," *Advances in Colloid and Interface Science*, vol. 120, no. 1–3, pp. 47–56, 2006.
- [39] K. Y. Foo and B. H. Hameed, "Insights into the modeling of adsorption isotherm systems," *Chemical Engineering Journal*, vol. 156, no. 1, pp. 2–10, 2010.
- [40] M. Ahmad, S. S. Lee, A. U. Rajapaksha et al., "Trichloroethylene adsorption by pine needle biochars produced at various pyrolysis temperatures," *Bioresource Technology*, vol. 143, pp. 615–622, 2013.



Journal of
Nanotechnology



International Journal of
Corrosion



International Journal of
Polymer Science



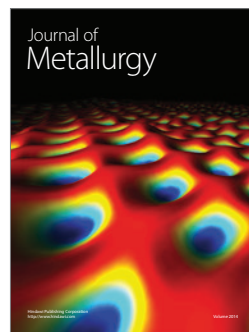
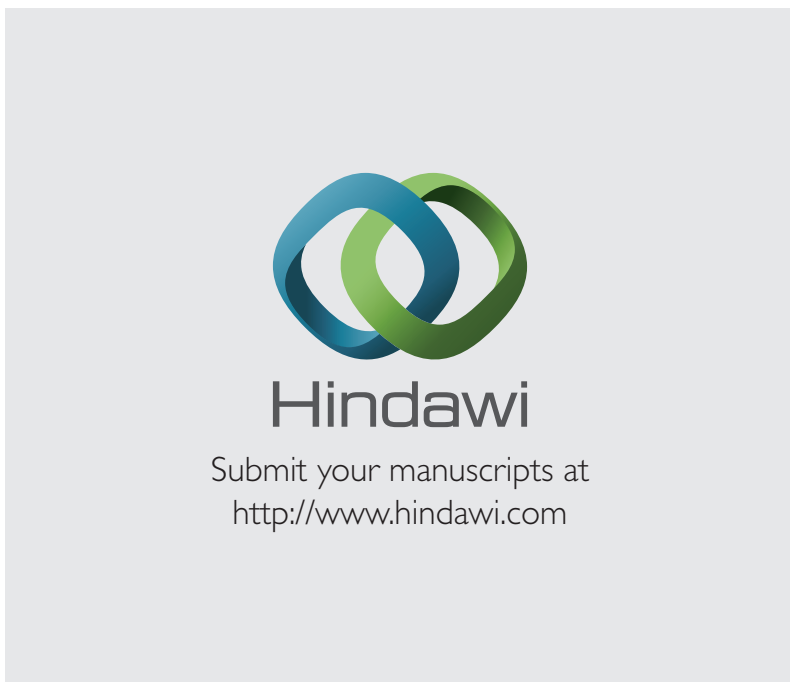
Smart Materials
Research



Journal of
Composites



BioMed
Research International



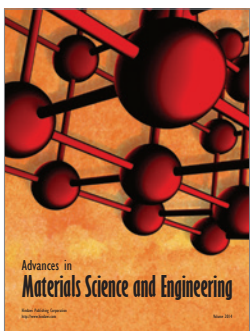
Journal of
Metallurgy



Journal of
Materials



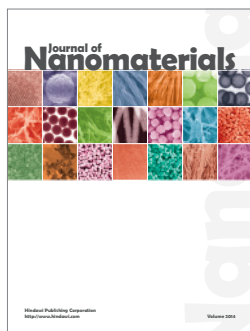
Journal of
Nanoparticles



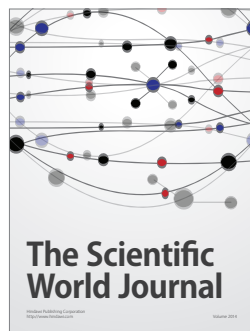
Advances in
Materials Science and Engineering



Scientifica



Journal of
Nanomaterials



The Scientific
World Journal



International Journal of
Biomaterials



Journal of
Nanoscience



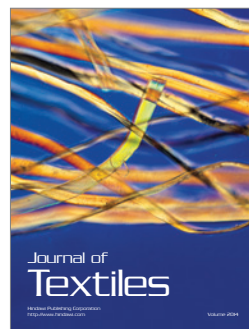
Journal of
Coatings



Journal of
Crystallography



Journal of
Ceramics



Journal of
Textiles